Insect swarms can be bound together by repulsive forces

A.M. Reynolds

Rothamsted Research, Harpenden, Hertfordshire, AL5 2JQ, UK.

Abstract The cohesion of insect swarms has been attributed to the fact that the resultant internal interactions of the swarming insects produce, on the average, a centrally attractive force that acts on each individual. Here it is shown how insect swarms can also be bound together by centrally forces that on the average are repulsive (outwardly directed from the swarm centres). This is predicted to arise when velocity statistics are heterogeneous (position-dependent). Evidence for repulsive forces is found in laboratory swarms of *Chironomus riparius* midges. In homogeneous swarms, the net inward acceleration balances the tendency of diffusion (stochastic noise) to transport individuals away from the centre of the swarm. In heterogenous swarms, turbophoresis – the tendency for individuals to migrate in the direction of decreasing kinetic energy – is operating. The new finding adds to the growing realization that insect swarms are analogous to self-gravitating systems. By acting in opposition to central attraction (gravity), the effects of heterogeneous velocities (energies) are analogous to the effects of dark energy. The emergence of resultant forces from collective behaviours would not be possible if individual flight patterns were themselves unstable. It is shown how individuals reduce the potential for the loose of flight control by minimizing the influence of jerks to which they are subjected.

Tel: +44 (0)1582 763133

Fax: +44 (0)1582 760981

Email: andy.reynolds@rothamsted.ac.uk

PACS 87.23.Ge - Dynamics of social systems

PACS 05.10.Gg – Stochastic analysis methods (Fokker-Planck, Langevin etc.)

Introduction

In contrast with bird flocks, fish schools and migratory herds, sparse swarms of flying insects do not possess global order but are, nonetheless, a form of collective animal behaviour [Okubo 1986, Kelley and Ouellette 2013]. The collective behaviour is evident in their emergent macroscopic mechanical properties. Laboratory swarms of *Chironomus riparius* midges, for example, have macroscopic mechanical properties similar to solid, including a finite Young's modulus and yield strength [Ni and Ouellette 2016]. The collective behaviour of these swarms is also evident in their response to dynamic illumination perturbations. The swarm-level response can be described by making an analogy with classical thermodynamics, with the state of the swarm moving along an isotherm in a thermodynamic phase plane [Sinhuber et al. 2019a]. Applied oscillatory visual stimuli induce a viscoelastic response as the perturbations are strongly dampened, both viscously and inertially [van der Vaart et al. 2019]. A distinctively different indicator of collective behavior lies in the composition of unperturbed swarms. Unperturbed laboratory swarms of *Chironomus riparius* midges consist of a core 'condensed' phase surrounded by a dilute 'vapour' phase [Sinhuber and Ouellette 2017]. Although these two phases have distinct macroscopic properties, individuals move freely between them, suggesting that they are collective, emergent states. The collective behaviours of laboratory swarms of *Chironomus riparius* midges are predicted by stochastic trajectory simulation models [Reynolds et al. 2017, Reynolds 2018a, 2019a,b, van der Vaart et al. 2019, 2020]. This and other modelling [Gorbonos et al. 2016, 2020, Reynolds 2019b] have also uncovered striking similarities between insect swarms and self-gravitating systems such as globular clusters, as foreseen by Okubo [1986]. Okubo [1986] noted that if the internal forces between individuals were like Newtonian gravitational attraction, then the resultant attraction on an individual within a uniform spherical swarm would be directly proportional to the distance from the swarm centre, as observed [Okubo 1986, Kelley and Ouellette 2013] and as predicted by the stochastic models.

To date, stochastic trajectory simulation models have been formulated for homogeneous swarms with position-independent velocity statistics. Here models are formulated for swarms with heterogeneous velocity statistics. The effects of heterogeneous velocity statistics are shown to be analogous to 'dark energy' causing individuals, on the average, to accelerate outwardly from the swarm centre. The outward accelerations need a supply of energy which for "active particles" like insects can be got from converting (unseen) internal energy into kinetic energy. Model predictions are supported by the results of numerical simulations and by analysis of pre-existing data for laboratory swarms of *Chironomus riparius* midges [Sinhuber et al. 2019b].

Swarm stability is contingent on the stability of individual trajectories. Modelling and data analysis reveal that individuals minimize the influence of potentially destabilizing jerks (changes in acceleration) to which they are subjected. I show that jerks along with an analogue of the Reynolds number appear in higher-order (generalized) stochastic models.

Model formulation and predictions

Here following Okubo [1] I assume that the positions, *x*, and velocities, *u*, of individual insects within a swarm can be described by the stochastic differential equations

$$dx = udt$$

$$du = a(u,x,t)dt + bdW(t) \quad (1)$$

where $dW(t)$ is an incremental Wiener process with correlation property $\overline{dW(t)dW(t+\tau)} = \delta(\tau)dt$. Such 1-dimensional, individual-based models are effectively first-order autoregressive stochastic processes in which positions and velocities are modelled as a joint Markovian process. At second-order, positions, velocities and accelerations are modelled collectively as a Markovian process. Physically, the hierarchy of stochastic models corresponds to the inclusion of a velocity autocorrelation timescale, *T*, at first order, and to the addition of an acceleration autocorrelation timescale, t_A, at second order and so on [Sawford 1991]. Continuum models of the kind pioneered by Bertozzi and Topaz [2004] and utilized, for example, by Topaz et al. [2012] are not appropriate because the Knudsen number Kn~O(1) [Puckett et al. 2014]. In the laboratory, *Chironomus riparius* midges appear somewhat paradoxically to be tightly bound to the swarm while at the same time weakly coupled inside it [Puckett et al. 2014].

Here the deterministic term, $a(u,x,t)$, is determined by the requirement that the statistical properties of the simulated trajectories be consistent with the observations of Kelley and Ouellette [2013] who reported on the position and velocity statistics of individual *Chironomus riparius* midges within laboratory swarms. Mathematically these consistency conditions require that the joint distribution of velocity and position $p(u,x,t)$ be a solution of the Fokker-Planck equation

$$\frac{\partial p}{\partial t} + u\frac{\partial p}{\partial x} = -\frac{\partial}{\partial u}(ap) + \frac{b^2}{2}\frac{\partial^2 p}{\partial u^2} \quad (2)$$

Here, in broad agreement with the observations of Kelley and Ouellette [2013], I assume that positions and velocities are statistically stationary and Gaussian distributed,

$$p(u,x) = \frac{1}{2\pi\sigma_x\sigma_u} exp\left(-\frac{x^2}{2\sigma_x^2}\right) exp\left(-\frac{u^2}{2\sigma_u^2}\right) \quad (3)$$

where σ_x is the root-mean-square position (i.e., the root-mean-square swarm size), and σ_u is the position-dependent root-mean-square speed. Equation 2 implies

$$ap = \frac{b^2}{2}\frac{\partial p}{\partial u} + \phi(x,u,t)$$

where for statistically stationary swarms having, $\frac{\partial p}{\partial t} = 0$, the quantity ϕ is determined by

$$\frac{\partial \phi}{\partial u} = -u\frac{\partial p}{\partial x}, \quad i.e., \quad \phi = -\frac{\partial}{\partial x}\int_{-\infty}^{u} updu \quad (4)$$

It follows from Eqns. 2, 3 and 4 that

$$du = -\frac{u}{T}dt - \frac{\sigma_u^2}{\sigma_x^2}xdt + \frac{1}{2}\left(1+\frac{u^2}{\sigma_u^2}\right)\frac{d\sigma_u^2}{dx}dt + \sqrt{\frac{2\sigma_u^2}{T}}dW \quad (5)$$

when, without loss of generality and on dimensional grounds, $b = \sqrt{\frac{2\sigma_u^2}{T}}$ where T is a model timescale. Details of the derivation of such models can be found in Thomson [1987]. The first term in Eqn. 5 is a 'memory term' which causes velocity fluctuations to relax to their mean value. The second and third terms are a conditional mean acceleration (restorative force). The fourth term is the stochastic driving noise. This accounts for fluctuations in the restorative force which arise because of the limited number of individuals in the swarm and because of nonuniformity in their spatial distribution [Okubo 1986]. Utilizing the continuous Fokker Planck equation, Eqn. 2, to determine the functional form of the discrete models, Eqn. 1., in the above way contrasts with the continuum formulation of fully-fledged discrete models of dense swarms [Chuang et al. 2007].

When velocities are homogeneous (i.e., when $\frac{d\sigma_u^2}{dx} = 0$), the model, Eqn. 5, reduces to Okubo's model [1986]. In this case, mean accelerations are directed towards the swarm centre and increase linearly with distance from the swarm centre, in accordance with observations

made at the cores of laboratory swarms [Okubo 1986, Kelley and Ouellette 2013]. This is consistent with insect swarms behaving as self-gravitating systems [Okubo 1986].

More generally, the velocity-averaged mean acceleration

$$\langle A|x\rangle = -\frac{\sigma_u^2}{\sigma_x^2}x + \frac{d\sigma_u^2}{dx} \tag{6}$$

Concave mean-square-velocity profiles therefore counteract with the linear term, $-\frac{\sigma_u^2}{\sigma_x^2}x$, (more generally $\sigma_u^2\frac{d\rho}{dx}$ where ρ is the aerial density profile) and if strong enough can overwhelm it completely so that mean accelerations are everywhere direct away rather than towards the swarm centre. Such swarms are therefore effectively bound together by repulsive forces.

Comparisons with simulation and experimental data

Individual trajectories were simulated by numerically integrating the stochastic model, Eqn. 1 and 5. Statistically stationary predictions for mean accelerations, velocity variances and spatial distributions were obtained from 100,000 simulated trajectories. The results of these numerical simulations confirm that swarms remain localized and coherent even though individuals are, on the average, accelerating outwardly away from the swarm centre. This is illustrated in Fig. 1 for the case when $\sigma_u^2 = \sigma_0^2\,\mathrm{e}^{x^2/\sigma_x^2}$ for $|x| < 2\sigma_x$ otherwise $\sigma_u^2 = \sigma_0^2\,\mathrm{e}^4$ so that $\langle A|x\rangle = \frac{\sigma_0^2}{\sigma_x^2}x$ for $|x| < 2\sigma_x$ otherwise $\langle A|x\rangle = 0$ Cases where individuals are everywhere, on the average, repulsive are non-physical because such swarms possess infinite kinetic energy. Further support, for the model predictions comes from an analysis of the pre-existing data for 3-dimensional swarms of *Chironomus riparius* midges [Sinhuber et al. 2019b]. Mean-square velocities within the cores of these swarms are position-independent and, as predicted, mean accelerations increase linearly with distance from the swarm centers (Fig. 2). In the outskirts of the swarms the concave shape of mean-square velocity profiles become apparent as does the expected associated weakening of the central attraction (due to contributions to the net resultant forces from repulsive forces).

Jerks and Reynolds numbers

Male midges swarm to provide a mating target for females, making stationarity desirable. Ni and Ouellette [2016] were the first to show that this biological function is reflected in an emergent physical macroscopic property of the swarm; namely its tensile strength. van der Vaart et al. [2019] subsequently showed that midge swarms also strongly dampen perturbations, both viscously and inertially. These findings suggest that midge swarms use their collective behaviour to stabilize themselves against environmental perturbations. Perturbations are inevitable in natural swarms that must contend with gusts of wind and with other environmental disturbances. Collective behavours can, however, only be stablizing if individual's trajectories are themselves stable. To avoid losing control of their body motion, it is not only necessary to limit the maximum acceleration, i.e., the force, an individual can be exposed to, but also the maximum jerk strength (rate of change of acceleration, $\frac{d^3x}{dt^3}$), since individuals need time to adjust to stress changes. Here I show that midges minimize the impact of jerks.

Jerks arise in second-order autoregressive models for the joint evolution of an individual's position, x, velocity, v, and acceleration, A:

$$\begin{aligned} dA &= a(A,u,x,t)dt + bdW(t) \\ du &= Adt \\ dx &= udt \end{aligned} \tag{7}$$

The formulation of such models mirrors closely that of first-order models, Eqn. 1. The position, velocity and accelerations of the simulated trajectories will be consistent with the observed form of the joint distribution of acceleration, velocity and position, $P(A,u,x,t)$, when $P(A,u,x,t)$ is a solution of the Fokker-Planck equation

$$\frac{\partial P}{\partial t} + u\frac{\partial P}{\partial x} + A\frac{\partial P}{\partial u} = -\frac{\partial}{\partial A}(aP) + \frac{b^2}{2}\frac{\partial^2 P}{\partial A^2} \tag{8}$$

Equation 8 implies that

$$a = \frac{b^2}{2}\frac{\partial \ln P}{\partial A} + \frac{\phi}{P} \tag{9}$$

where for statistically stationary swarms having, $\frac{\partial P}{\partial t} = 0$,

$$\frac{\partial \phi}{\partial A} = -u\frac{\partial P}{\partial x} - A\frac{\partial P}{\partial u} \tag{10}$$

The first term on the right-hand side of Eqn. 10 a memory term which causes accelerations to relax to their mean value, $\langle A \rangle$. The second term on the right-hand side $\frac{\phi}{P}$ of Eqn. 9 is the mean jerk strength $\langle J \rangle$. It follows from Eqn. 10 that when accelerations, velocities are homogeneous (position independent) and Gaussian distributed, the mean jerk strength

$$\langle J \rangle = u\left(\frac{\partial \langle A \rangle}{\partial x} - \frac{\sigma_A^2}{\sigma_u^2} \right) \tag{11}$$

An equation for the mean acceleration – identical to Eqn. 4 - is obtained from Eqn. 10 after integrating over all accelerations. For swarms with Gaussian density profiles, $\langle A \rangle = -\frac{\sigma_u^2}{\sigma_x^2} x$. In accordance with Eqn. 11, the mean jerk strength is observed to increase linearly with velocity when velocities lie within the Gaussian cores of the velocity distributions (Fig. 3a). Discrepancies between the predicted and observed mean jerk strengths only become significant at higher velocities, $|u| > 2\sigma_u$, which lie within the exponential tails of the velocity distribution [Kelley and Ouellette 2013] and so beyond the scope of the model. Moreover, as predicted, the average observed jerk strength does not vary significantly with position in the swarm (Fig 3b). Model predictions for velocity-averaged jerk strengths $\left| \langle J(u > 0) \rangle \right|$ are also in good agreement with data for a variety of laboratory swarms with mean sizes between 19 and 94 individuals (Fig. 3c). The simple, 1-dimensional model is seen to *consistency* overpredict $\left| \langle J(u > 0) \rangle \right|$ by a factor of about 3/2.

The above analysis is readily extended from 1 and 3-dimensions and to thereby account for velocity covariances. In this case

$$\langle J_i \rangle = -u_j \left(\frac{\langle u_i u_j \rangle}{\sigma_x^2} + \sigma_A^2 \tau_{ij} \right) \tag{12}$$

where the subscripts denote Cartesian coordinates and where τ is the inverse of the velocity covariance matrix $\langle u_i u_j \rangle$. The mean jerks are therefore aligned with the direction of travel, i.e., with the body axis, when the velocity covariances vanish. This has resonance with Reynolds

et al. [2016] who suggested that migratory insects use turbulence-induced jerks as an indication of mean wind direction when flying at altitude. The average magnitude of the jerks is smallest along the mean wind line (or to right of the mean wind line in Ekman spiral atmosphere in the Northern Hemisphere). Vanishing velocity covariances are not inevitable. Analysis of the datasets of Sinhuber et al. [2019b] of laboratory swarms of midges, for example, reveals that velocity covariances are non-zero but 10 to 20 times smaller than the velocity variances. And, as predicted, mean jerks are found to be effectively aligned with velocity.

An analogue of the Reynolds number, which is determined by the ratio of T and t_A, $\mathrm{Re}^* = \left(T / t_A\right)^2$, appears as a parameter at second order [Sawford 2003]. This provide a new way to characterise swarm behaviours. Indeed, modelling predicts a transition from under- and over-damped movements with increasing Reynolds number (Fig. S1).

More elaborate models

In principle the modelling could be extended to account for distributions of acceleration having heavy tails [Kelley and Ouellette 2013]. It should, however, be noted that the naïve approach of simply specifying non-Gaussian accelerations produces non-physical effects in stochastic modelling of tracer-particle trajectories in turbulence [Reynolds 2003a]. More realistic stochastic models of tracer-particle trajectories in turbulence are formulated in terms of conditional distributions of accelerations under the assumption that these are Gaussian [Reynolds 2003b, Reynolds et al. 2005, Lamorgese et al. 2007]. Tracer-particle accelerations have a conditional dependency on both the rate of dissipation of turbulent kinetic energy and velocity [Sawford et al. 2003]. Likewise, the mean accelerations of swarming insects are velocity dependent [Reynolds et al. 2017], as are the acceleration variances, $\sigma_A^{\,2}\left(u,x\right)$ (Fig. 4a). The latter implies that large fluctuations in acceleration tend to be associated with large velocities. The correlation between the square of the fluctuations in accelerations and square of velocity is small but not negligible (the correlation coefficient, $\rho_{A^2u^2} = \dfrac{\left\langle A^2u^2\right\rangle - \left\langle A^2\right\rangle\left\langle u^2\right\rangle}{\left(\left\langle A^4\right\rangle - \left\langle A^2\right\rangle^2\right)^{1/2}\left(\left\langle u^4\right\rangle - \left\langle u^2\right\rangle^2\right)^{1/2}} \sim 0.1$). Fluctuations in acceleration are, therefore, just as likely to reinforce the velocity as they are to oppose it. The data for $\sigma_A^{\,2}\left(u,x\right)$ are seen to be equally well represented by $\sigma_A^2 = a_0 + a_4u^4$ and by $\sigma_A^2 = a_0 + a_6u^6$ (Fig. 4a). The velocity

dependency of the acceleration variances may be attributed to insect trajectories occasionally rotating [Reynolds 2019b]. An insect will complete a half a rotation (of radius r) and change its velocity by an amount $\Delta u = 2u$ in a time $\tau = \pi r / |u|$. Consequently, acceleration variances $\left\langle \left(\frac{\Delta u}{\tau} \right)^2 \right\rangle \sim u^4$ when $u \sim r^0$ and $\sim u^6$ when $u \sim r^{-1}$. If $u \sim r^{-1}$ then an insect will not rotate over itself: it will maintain the same orientation while circulating behaving like a passive particle in an irrotational produced by a vortex tube. It is interesting to note that the acceleration variances of passive tracer-particles in turbulence and those of simulated passive tracer-particles of direct numerical simulations also have a u^6 dependency which has been attributed to rotations (around vortex filaments) [Mordant et al. 2004, Sawford et al. 2003]. As with the case of turbulence [Sawford et al. 2013], the velocity-dependent accelerations variances may account for distributions of acceleration having heavy tails [Kelley and Ouellette 2013] (Fig. 4b) and for the collapse of the conditional distributions $P\left(A|u\right)$ (Fig. 4c). Following Sawford *et al.* [2013], a heuristic understanding of this relationship can be attained by assuming that conditional distributions of acceleration are Gaussian. For large accelerations, the unconditional distribution of accelerations, $P\left(A\right) = \int_{-\infty}^{\infty} P\left(A|u\right) p\left(u\right) du$ can be evaluated using the saddle point approximation. If, as observed [Kelly and Ouellette 2013], velocity distributions have long exponential tails, then the saddle point approximation gives $P\left(A\right) \sim \exp\left(-\alpha A^{\frac{2}{1+p}} \right)$ where α is a constant. Laboratory results for the distribution acceleration are well represented by $P = N \exp\left(-\frac{A^2}{\left(\alpha + \beta |A|^2 \right)^{6/7}} \right)$ where N is a normalization constant and where α and β are constants (Fig.4c). This ansatz has a Gaussian core and a stretched exponential tail. The model exponent for the tail, $2/\left(1+p\right)$, matches the empirical value, 2/7, when $p=6$. It may be difficult to improve on this model. Note also that these intrinsic fluid-like properties of swarming midges in still air may, like other properties of swarming midges, be modified if the air itself is set in motion or if the swarm is perturbed in other ways by external perturbations [Sinhuber et al. 2019a, van der Vaart et al. 2020]; mirroring expectations for swarming in viscous fluids [Chuang et al. 2016].

Discussion

Here I reported on the first theoretical analysis of heterogeneous insect swarms with position-dependent velocity statistics. The analysis demonstrated the utility of a model formulation which has proved to be highly effective when applied to homogeneous swarms [Reynolds et al. 2017, Reynolds 2018a, 2019a,b, van der Vaart 2019, 2020]. It revealed how heterogeneous velocity statistics $\frac{d\sigma_u^2}{dx}$ contribute to mean accelerations, $\langle A|x \rangle$, countering or even overwhelming centrally-attractive accelerations, $-\frac{\sigma_u^2}{\sigma_x^2}x$ (Eqn. 5)**.** The former was evident in the results of numerical simulations (Fig.1) which confirmed that individuals can be bounded to the swarm centre by a resultant force that, on the average, is repulsive; a seemingly paradoxical situation. Evidence for repulsive forces was uncovered in an analysis of pre-existing experimental data (Fig. 2). The mechanism is clear. In homogeneous swarms, the net inward acceleration balances the tendency of diffusion (stochastic noise) to transport individuals away from the centre of the swarm. In heterogenous swarms, turbophoresis is operating. If, as is observed (Fig. 2), $\sigma_u^2(x)$ is concave, then in statistically-stable swarms this tendency of individuals to move inwards towards to centres of swarms must be countered by net outward accelerations. Concave velocity-variance profiles together with the assumption that velocities are locally Gaussian also accounts for the observed presence of velocity distributions with long-exponential tails [Kelley and Ouellette 2013, Reynolds 2019b]. This juxtaposition also accounts for the observed occurrence of speed-dependent forces, Eqn. 5 [Reynolds et al. 2017]. Concave velocity-variance profiles are predicted by the mechanistic models which attribute swarm cohesion to the sporadic and temporary formulation of bound pairs of individuals flying in synchrony [Reynolds 2019b], as observed by Puckett et al. [2015]. They may be also attributed to the influence of the ground-based visual features known as swarm markers [Puckett and Ouellette 2014] or result from interactions between swarming insects and faster insects outside of the swarms [Puckett and Ouellette 2014]: interactions that may also account for the presence of stabilizing inwards effective pressure on the surface of the swarms [Gorbonos et al. 2016].

Okubo [1986] speculated that insect swarms are analogous to self-gravitating systems and therefore individuals are attracted to the centre of the swarm by an effective net force that increases linearly with distance from the swarm centre. There is now strong experimental support for such a net linear restoring force operating within the cores of laboratory swarms [Kelley and Ouellette 2013]. More recent studies have uncovered more striking analogies with

self-gravitating systems: including the occurrence of polytropic distributions (which constitute the simplest, physically plausible models for self-gravitating stellar systems), together with biological correlates of Jean's instabilities, black hole entropies, Mach's Principle, surface pressures, and dark matter [Gorbonos et al. 2016, Gorbonos and Gov 2017, Gorbonos et al. 2020, Reynolds 2018b, 2019b, Supplementary Material]. By providing a revision to Okubo [1986] I have uncovered another biological correlate of self-gravitating systems: namely dark energy. In analogy with dark energy, heterogenous velocity statistics were shown to act to opposition to the net inward force identified by Okubo [1986]. This opposition becomes significant in the outskirts of swarms. The enrichening of the analogy with self-gravitating systems compliments ongoing attempts to establish a 'thermodynamic' understanding of swarming [Ouellette 2017, Sinhuber et al. 2019] A complete understanding of the collective behaviour of insect swarms may ultimately be found in both their emergent macroscopic mechanical and thermodynamic properties, and in their similitude with self-gravitating systems. The emergence of these properties is contingent on individuals not losing control of their trajectories. It was shown how individuals in the swarms reduce the potential for the loose of flight control by minimizing the potentially destabilizing influences of jerks; mirroring expectations for migratory insects [Reynolds et al. 2016].

Finally, it was shown that an analogue of the Reynolds number appears as a parameter in second-order stochastic models, opening up a new unexplored avenue for characterizing collective behaviours [Smith et al. 2019].

Acknowledgements

The work at Rothamsted forms part of the Smart Crop Protection (SCP) strategic programme (BBS/OS/CP/000001) funded through the Biotechnology and Biological Sciences Research Council's Industrial Strategy Challenge Fund.

References

Chuang, Y-L., D'Orsogna, M.R., Marthaler, D., Bertozzi, A.L., & Chayes, L.S. State transitions and the continuum limit for a 2D interacting, self-propelled particle system. *Physica D* **232**, 33-47 (2007).

Chuang, Y-L., Chou, T. & D'Orsogna, M.R. Swarming in viscous fluids: Three-dimensional patterns in swimmer- and force-induced flows. *Phys. Rev. E* **93**, 043112 (2016).

Gorbonos, D., Ianconescu, R., Puckett, J. G., Ni, R., Ouellette, N. T. & Gov, N. S. Long-range acoustic interactions in insect swarms: an adaptive gravity model. *New J. Phys.* **18**, 073042 (2016).

Gorbonos, D. & Gov, N.S. Stable Swarming Using Adaptive Long-range Interactions. *Phys. Rev. E* **95**, 042405 (2017).

Gorbonos, D., van der Vaart, K., Sinhuber, M., Puckett, J.G., Ouellette, N.T., Reynolds, A.M., Gov, N.S. Similarities between insect swarms and isothermal globular clusters. *Phys. Rev. Res.* **2**, 013271 (2020).

Kelley, D.H. & Ouellette, N.T. Emergent dynamics of laboratory insect swarms. *Sci. Rep.* **3**, 1073, 1-7 (2013).

Lamorgese, A.G., Pope, S.B., Yeung, P.K. & Sawford, B.L. A conditionally cubic-Gaussian stochastic Lagrangian model for acceleration in isotropic turbulence. *J. Fluid Mech.* **582**, 423-448 (2007).

Mordant, N., Crawford, A.M. & Bodenschatz, E. Experimental Lagrangian acceleration probability density function measurement. *Physica D* **193**, 245-251 (2004).

Okubo, A. Dynamical aspects of animal grouping: swarms, schools, flocks and herds. *Adv. Biophys.* **22**, 1-94 (1986).

Ouellette, N.T. Toward a “thermodynamics” of collective behaviour. *SIAM News* (2017).

Puckett, J.G. & Ouellette, N.T. Determining asymptotically large population sizes in insect swarms. *J. Roy. Soc. Inter.* **11,** 20140710 (2014).

Puckett, J.G., Ni, R. & Ouellette, N.T. Time-frequency analysis reveals pairwise interactions in insect swarms. *Phys. Rev. Lett.* **114**, 258103 (2015).

Ni, R. & Ouellette, N.T. On the tensile strength of insect swarms. *Phys. Biol.* **13**, 045002 (2016).

Reeks, M.W. The transport of discrete particles in inhomogeneous turbulence, *J. Aerosol Sci*., **14**,729-739 (1983).

Reynolds, A.M. On the application of nonextensive statistics to Lagrangian turbulence. *Phys. Fluids* **15**, L1- (2003a).

Reynolds, A.M. On the superstatistical mechanics of tracer-particle motions in turbulence. *Phys. Rev. Lett.* **91**, article 84503 (2003b).

Reynolds, A.M., Mordant, N., Crawford, A.M. & Bodenschatz, E. On the distribution of Lagrangian accelerations in turbulent flows, *New J. Phys.* **7**, 58-67 (2005).

Reynolds, A.M., Sinhuber M. & Ouellette N.T. Are midge swarms bound together by an effective velocity-dependent gravity? *Euro. Phys. J. E* **40**,46 (2017).

Reynolds, A.M. Langevin dynamics encapsulate the microscopic and emergent macroscopic properties of midge swarms. *J. Roy. Soc. Inter.* **15**, 20170806 (2018a).

Reynolds, A.M. Fluctuating environments drive insect swarms into a new state that is robust to perturbations. *Europhys. Lett.* **124**, 38001 (2018b).

Reynolds, A.M. On the origin of the tensile strength of insect swarms. *Phys. Biol.* **16** 046002 (2019a).

Reynolds, A.M. On the emergence of gravitational-like forces in insect swarms. *J. Roy. Soc. Int.* **16,** 20190404 (2019b).

Reynolds A.M. & Ouellette N.T. Swarm dynamics may give rise to Lévy flights. *Sci. Rep.* **6**, 30515 (2016).

Reynolds A.M., Reynolds D., Sane S.P., Hu G. & Chapman J.W. Orientation in migrating insects in relation to flows: mechanisms and strategies. *Phil. Trans. Roy. Soc. B* **371**, 20150392 (2016).

Sawford, B.L. Reynolds number effects in Lagrangian stochastic models of turbulent dispersion. *Phys. Fluids A* **3**, 1577-1586 (1991).

Sawford, B.L., Yeung, P.K., Borgas, M.S., Vedula, P., La Porta, Crawford, A.M. & Bodenschatz, E. Conditional and unconditional acceleration statistics in turbulence. *Phys. Fluids **15**,* 3478-3489 (2003).

Sinhuber, M. & Ouellette, N.T. Phase coexistence in insect swarms. *Phys. Rev. Lett.* **119**, 178003 (2017).

Sinhuber, M., van der Vaart, K. & Ouellette, N.T. Response of insect swarms to dynamic illumination perturbations. *J. R. Soc. Interface* **16**, 20180739 (2019a).

Sinhuber, M., van der Vaart, K., Ni, R., Puckett, J.G., Kelley, D.H. & Ouellette, N.T. Three-dimensional time-resolved trajectories from laboratory insect swarms. *Sci. Data* **6**, 190036 (2019b).

Sinhuber, M., van der Vaart, K. Feng, Y., Reynolds A.M. & Ouellette, N.T. An equation of state for insect swarms. (2019c) (Submitted).

Smith, N.M., Dickerson, A.K. & Murphy, D. Organismal aggregations exhibit fluidic behaviors: a review. *Bioinspir. Biomim.* **14**, 031001 (2019).

Thomson, D.J. Criteria for the selection of stochastic models of particle trajectories in turbulent flows. *J. Fluid Mech.* **180**, 529-556 (1987).

Topaz, C.M. & Bertozzi, A.L. Swarming Patterns in a Two-Dimensional Kinematic Model for Biological Groups. *SIAM J. Appl. Math.*, **65**, 152–174 (2004).

Topaz, C.M., D'Orsogna, M.R., Edelstein-Keshet, L. & Bernoff A-J. Locust Dynamics: Behavioral Phase Change and Swarming. *PLoS Comp. Biol.* **8**, e1002642 (2012).

van der Vaart, K., Sinhuber M., Reynolds, A.M., Ouellette, N.T. Mechanical spectroscopy of insect swarms. *Sci. Adv.* **5**, eaaw9305. (2019).

van der Vaart, K., Sinhuber, M., Reynolds, A.M., Ouellette, N.T. Environmental perturbations induce correlations in midge swarms. *J. R. Soc. Interface* **17**, 20200018 (2020).

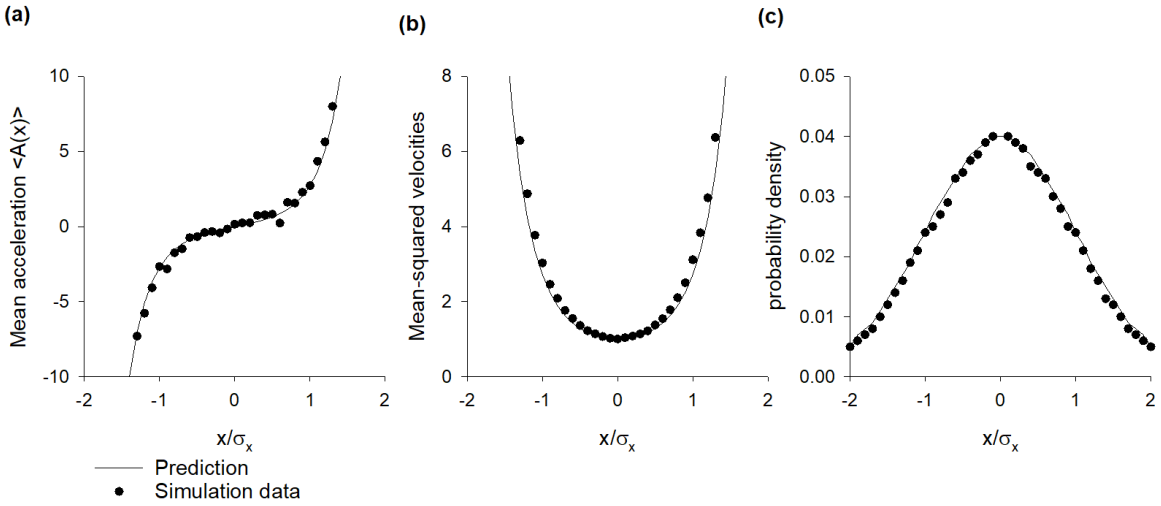

440

Figure 1. Insect swarms are predicted to remain localized and coherent even when every individual is, on the average, accelerating outwardly from the swarm centre. Individual trajectories were simulated using the stochastic model, Eqn. 1 and 5 with $\sigma_x^2 = 1, \sigma_u^2 = \sigma_0^2 \, \mathrm{e}^{x^2/\sigma_x^2}$ for $|x| < 2\sigma_x$ otherwise $\sigma_u^2 = \sigma_0^2 e^4$, $\sigma_0 = 1$ and $T = 1$ a.u. 100,000 individuals were simulated for a time *t=5* a.u. whereupon their positions, velocities and accelerations were recorded (●). Initial positions were Gaussian distributed with mean zero and variance σ_x^2. Initial velocities were Gaussian distributed with mean zero and variance $\sigma_u^2(x)$.

445

450

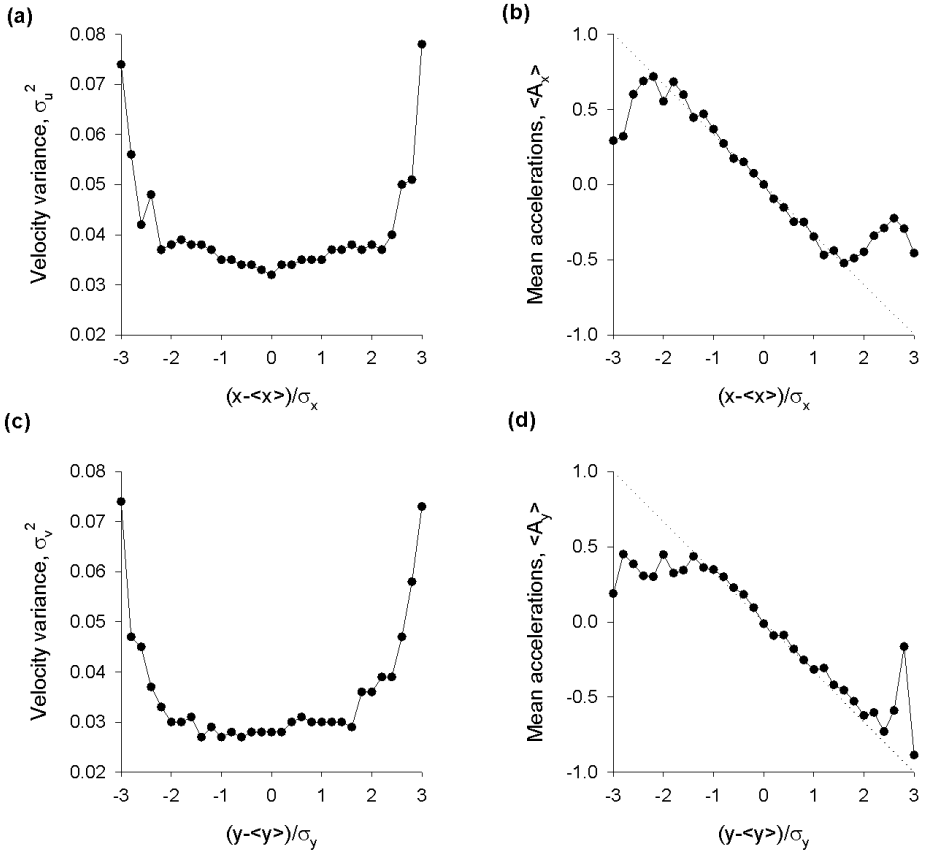

Figure 2. Hallmarks of model predictions in laboratory insect swarms. Concave velocity-variance profiles co-exist with suppressed inward accelerations (indicative of contributions from outward accelerations). Data are taken from Sinhuber et al. [2019b] for horizontal movements. Velocity variances and mean accelerations are ensemble averages over all 17 dusk time swarms in the dataset. To reduce the effects of meandering centres and fluctuations in swarm size, position-dependent velocity variances and mean accelerations were calculated for 10 s long runs of data. These quantities were then ensemble-averaged. Data for vertical movements is not shown because laboratory swarms are distorted in that direction by the presence of the ground, and because individuals tend to join the swarm by flying above it [Kelley and Ouellette 2013]. Also shown is the linear dependency of mean accelerations with distance from the swarm centre that is expected for homogeneous swarms (dashed lines).

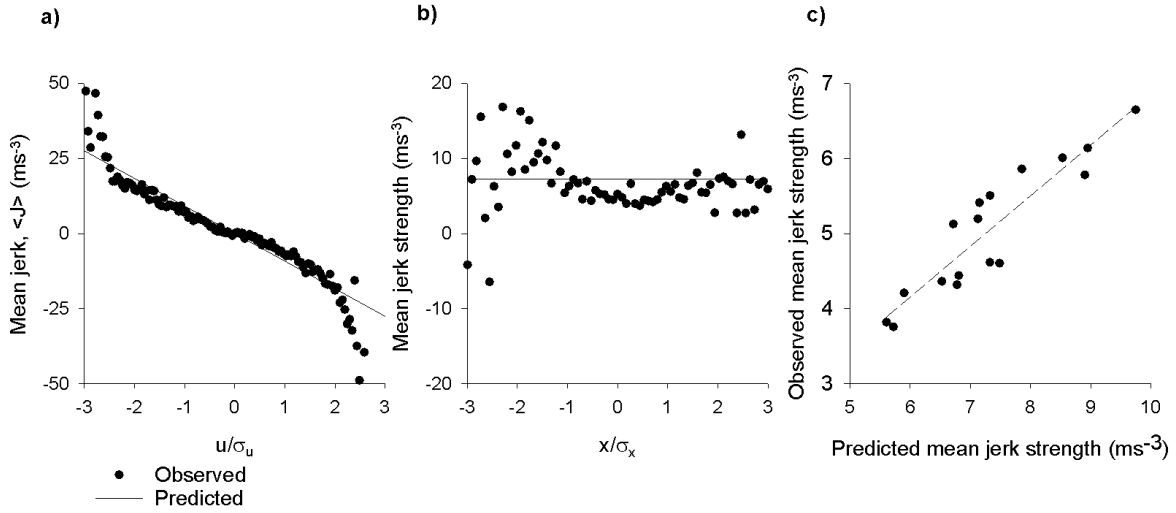

465

Figure 3 Comparisons of predicted and observed mean jerk strengths. An example comparison of the predicted and observed dependency of the mean jerk strength on a) velocity and b) position. Experimental data are taken from the smallest swarm (Ob17) in the data set of Sinhuber et al. [2019b]. In accordance with model expectations, Eqn. 11, the mean

470 jerk strength increases linearly with velocity according to $J = -u\left(\frac{\sigma_u^2}{\sigma_x^2} + \frac{\sigma_A^2}{\sigma_u^2}\right)$ and the mean jerk strength $\left|\left\langle J\left(u>0\right)\right\rangle\right| = \sqrt{\frac{2}{\pi}}\sigma_u\left(\frac{\sigma_u^2}{\sigma_x^2} + \frac{\sigma_A^2}{\sigma_u^2}\right)$ is independent of position. **c) Comparison of predicted and observed velocity-averaged jerk strengths** $\left|\left\langle J\left(u>0\right)\right\rangle\right|$**.** Experimental data are taken from all 17 dusk-time swarms in the data set of Sinhuber et al. [2019b]. The dashed-line is a least squares regression (R=0.93). Directly comparable results are obtained for the

475 y- and z- (vertical) directions. Experimental data are taken from all 17 dusk-time swarms in the data set of Sinhuber et al. [2019b].

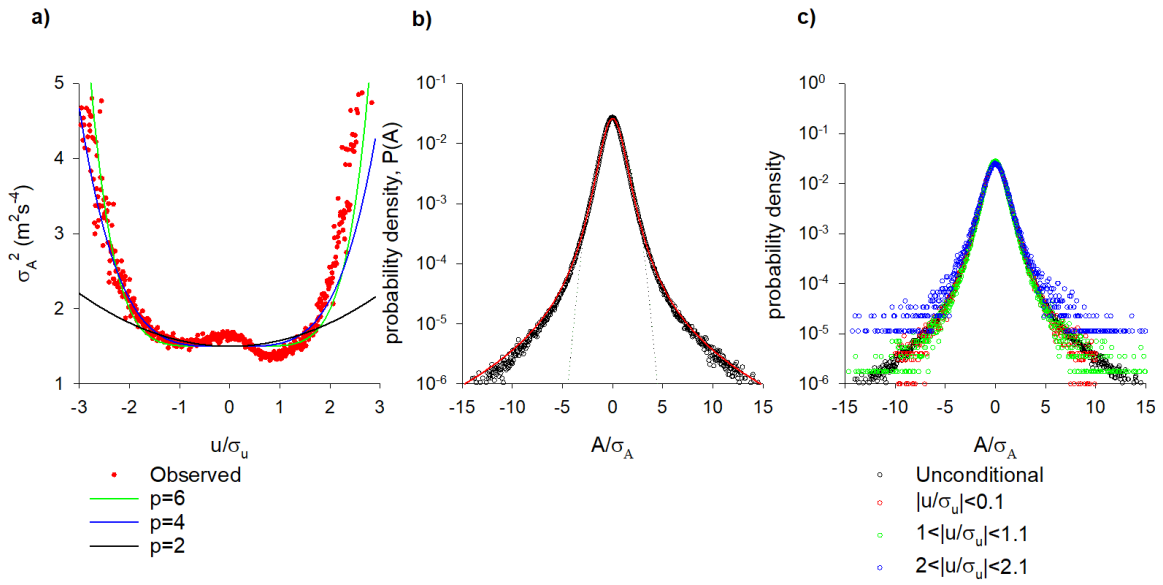

480 **Figure 4 a) Acceleration variances depend on velocity.** The lines are fits to $\sigma_A^2 = a_0 + a_p u^p$ with *p*=2, 4 and 6. Experimental data are taken from all 17 dusk-time swarms in the data set of Sinhuber et al. [2019b]. **b) Comparison of observed and predicted unconditional probability density functions (PDFs) of acceleration.** Experimental data are taken from all 17 dusk-time swarms in the data set of Sinhuber et al. [2019b] (black line) (one horizontal 485 component of acceleration). In accordance with model expectations the PDF has a heavy tailed compared with the Gaussian (dashed line). The data are very well represented by a stretched exponential $P(A) = N \exp\left(-\frac{A^2}{\left(\alpha + \beta |A|^2\right)^{6/7}}\right)$ where *N* is a normalization constant and where the constants *α* and *β* were determined by maximizing the associated log likelihood function. (red line) **c) Unconditional and conditional PDFs of acceleration have similar** 490 **shapes.** The observed collapse of the conditional PDFs suggests that the stretched exponential tails and the postulated power-law of the conditional acceleration variances may be related.

Supplementary Material

Reynolds number effects

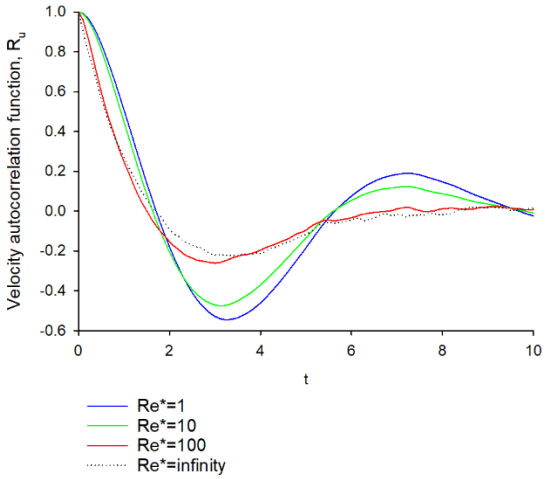

495

Figure S1. Swarms are predicted to transition from being underdamped to being overdamped as the effective Reynolds number increases. In the underdamped cases velocity autocorrelation functions are oscillatory and individual motions are pendulum-like, and in the overdamped case individual motions resemble a centrally biased random walk. 500 Simulation data was produced by the one-dimensional, second-order stochastic models, Eqn. 7-10, for swarms with positions, *x*, velocities, u, and accelerations, *A*, that are independent and Gaussian. Following Sawford [1991] the intensity of the stochastic noise $b^2 = 2\sigma_u^2\left(T^{-1} + t_A^{-1}\right)T^{-1}t_A^{-1}$. Model predictions were obtained for swarms with $\sigma_x^2 = 2, \sigma_u^2 = 1,\ T = 1$ (a.u.) and with $t_A = T / \mathrm{Re}^{*1/2}$. Predictions for $\mathrm{Re}^* \to \infty$ were 505 obtained using the one-dimensional, first-order stochastic model, Eqn. 5 with $\sigma_x^2 = 1, \sigma_u^2 = 1$ and $T = 1$. In this model, $\sigma_A^2 = \mathrm{Re}^{*1/2}\ \sigma_u{}^2 / T^2$.

Confirming essential elements of a 'dark matter halo' theory of surface pressures

The scalar virial theorem states that for a stable (statistically-stationary) self-gravitating system *2T+W+S=0* where *T* is the kinetic energy, *W* is the potential energy and *S* is the surface pressure. Here *T*, *W* and *S* are specific quantities. The potential energy $W = \left\langle \mathbf{A}.\mathbf{x} \right\rangle$ where **A** is the acceleration of an individual, and **x** is its position relative to the average position of the swarm centre. Gorbonos et al. [2016] found that laboratory swarms of the midge *Chironomus riparius* have S<0, indicating that the swarms are effectively experiencing stabilizing inward pressures on their outer surfaces. Reynolds [2018] proposed that the surface pressure is the result of the observed flux of individuals into and out of the swarm [Kelley and Ouellette 2012, Ni and Ouellette 2016, Sinhuber et al. 2019]. According to Reynolds [2018] this flux causes sporadic (mean zero) movements of the swarm's centre-of-mass, $\bar{\chi}$ which result in a surface pressure term given by $S = -\left\langle \mathbf{U}^2 \right\rangle$ where $\mathbf{U} = \frac{d\bar{\mathbf{x}}}{dt}$. In the analogy with self-gravitating systems, the predicted contributions to the swarm binding from the surrounding insects correspond to a 'dark matter halo'; structures that extended well beyond the edges of stellar systems and those existence can be inferred through their effects on the motions of stars and gas within those systems.

Here I provide the first evidence in support of the theory of Reynolds [2018] through analysis of the datasets of Sinhuber et al. [2019]. The number of individuals within a swarm fluctuates over time. To good approximation (R^2=0.79) the size of these fluctuations σ_n increases with the average swarm size, *n* (Fig. S2a). This may be an example of Taylor's [1961] law (known as fluctuation scaling in the physics literature) which posits that $\sigma_n = an^b$ where *b* is a species-specific aggregation index. Centre-of-mass movements increase with increasing σ_n (Fig. S2b). And to good approximation, $S = -\left\langle \mathbf{U}^2 \right\rangle$ (Fig. S2c) in accordance with theoretical expectations [Reynolds 2018]. The surface pressure was calculated from the scalar virial theorem. By way of contrast no evidence was found for what is perhaps the simplest explanation for S<0; namely for the co-existence of bound individuals with *2T+W=0 (S=0*) and free (unbound) individuals with *T>0*, *W=0* (effectively corresponding *S<0*).

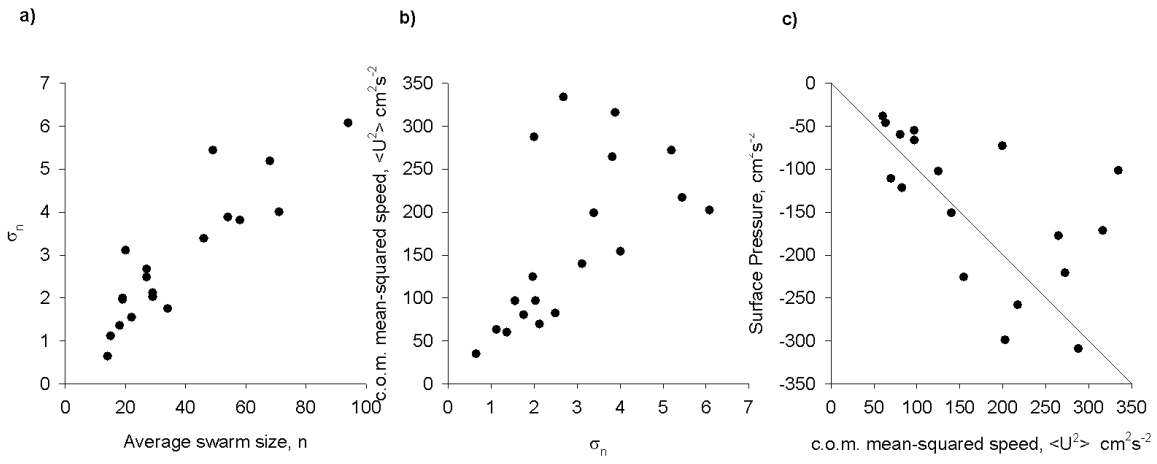

Figure S2. Analysis of the laboratory swarms of the midge *Chironomus riparius* is consistent with the theoretical analysis of Reynolds [2018]. a) Fluctuations in swarm size σ_n increase with swarm size. **b)** Centre-of-mass (c.o.m.) movements increase with σ_n. **c)** To good approximation $S = -\left\langle \mathbf{U}^2 \right\rangle$, in accordance with theoretical expectations [Reynolds 2018]. Data are taken from Sinhuber et al. [2019].

References

Kelley, D.H. & Ouellette, N.T. Emergent dynamics of laboratory insect swarms. *Sci. Rep.* **3**, 1073, 1-7 (2013).

Ni, R. & Ouellette, N.T. On the tensile strength of insect swarms. *Phys. Biol.* **13**, 045002 (2016).

Reynolds, A.M. On the emergence of gravitational-like forces in insect swarms. *J. Roy. Soc. Int.* **16,** 20190404 (2019).

Sawford, B.L. Reynolds number effects in Lagrangian stochastic models of turbulent dispersion. *Phys. Fluids A* **3**, 1577-1586 (1991).

Sinhuber, M., van der Vaart, K., Ni, R., Puckett, J.G., Kelley, D.H. & Ouellette, N.T. Three-dimensional time-resolved trajectories from laboratory insect swarms. *Sci. Data* **6**, 190036 (2019).

Taylor, L. R. Aggregation, variance and the mean. *Nature* **189**, 732–735 (1991).